

CO12-1 Determination of natural cobalt content as impurity in iron cyclotron yokes

G. Yoshida, K. Nishikawa¹, K. Takahashi, H. Nakamura, H. Yashima², M. Inagaki², S. Sekimoto², T. Miura, A. Toyoda, H. Matsumura, and K. Masumoto

Radiation Science Center, KEK

¹ Quantum Life and Medical Science Directorate, QST

² Institute for Integrated Radiation and Nuclear Science, Kyoto University

INTRODUCTION: In Japan, the number of establishment of accelerator facility had increased rapidly since the 1990s. Most of them are cyclotrons for Positron Emission Tomography (PET) drug production and are expected to be decommissioned in the near future, considering their useful life. When the decommissioning of accelerators, the generation of radioactive waste resulting from activation and their disposal become significant issue. Therefore, it is important to quantify the degree of activation in the whole facility, and it can predict the amount of generated radioactive waste accurately in order to facilitate decommissioning.

We focused on the iron yoke of PET cyclotron which accounts for a large amount of weight in the facility, and developed the activation estimation tool using Monte Carlo simulation. In this method, 3D-model which can reproduce the actual cyclotron is established and the rate of nuclear reactions for each modeling element is calculated by PHITS [1]. As a pilot study for this method, we performed the calculation for the PET cyclotron at the Nishina Memorial Cyclotron Center (NMCC) in the Takizawa Research Institute of the Japan Radioisotope Association in Takizawa City, Iwate Prefecture. The calculated reaction rate gradient agreed well with the radioactivity depth gradient of the actual yoke determined by the core boring method. However, we could not discuss whether the absolute values of radioactivity are consistent or not because the concentration of cobalt which content as impurity in the iron yoke has not been quantified.

In this study, we analyzed trace element concentrations in some iron and steel samples with neutron activation analysis (NAA) which suitable for trace element analysis of ppm order. We have been used NAA for quantification of trace elements in accelerator facility concretes [2], though this is the first time to apply this method for metallic materials. The feasibility of NAA for determination of trace elements in the steel sample was also verified in this study.

EXPERIMENTS: Irradiation samples were prepared from iron yoke of PET-cyclotron in NMCC. Chips were taken from the surface layer where no activation was observed, using a drill. Iron chips were washed with boiled water twice and with acetone, then dried and weighed by 100 mg as an irradiation sample. Japanese iron and steel certified reference materials (JSS001-8, JSS003-7, JSS050-8, JSS651-16, JSS-652-16) distributed by the

Japan iron and steel federation were employed as references and prepared in the same way. For analysis of short-lived nuclides generated by neutron irradiation, samples were irradiated at Pn-3 with 1 MW during 10 s, and measured with a Ge detector immediately after irradiation. Next day of 10s irradiation, samples were irradiated at Pn-2 with 5 MW during 3000 s, and measured with a Ge detector after short lived nuclides were attenuated.

RESULTS: The results of the 10s irradiation showed ⁵⁶Mn and ²⁸Al peaks in the γ -ray spectra of all samples. Relative value of radioactivity was consistent with the nominal values of manganese and aluminum in the standard sample. We measured the 3000s irradiated samples with a Ge detector one month after irradiation. The result of the long time irradiation showed ⁵⁹Fe and ⁶⁰Co peaks in the γ -ray spectra of all samples, though that in some samples the ⁵⁹Fe peak was too large and masked the ⁶⁰Co peak. Remeasurement of these samples after the ⁵⁹Fe had decay enough are mandatory.

The cobalt concentration in the iron yoke of the NMCC cyclotron was estimated to be approximately 40 μ g/g. From this value and the ⁶⁰Co reaction rate, the radioactivity distribution was derived as shown in Fig.1 and agreed very well with the actual radioactivity depth distribution. In conclusion, it was found that aluminum, manganese, and cobalt in iron samples in an accelerator can be determined accurately using NAA.

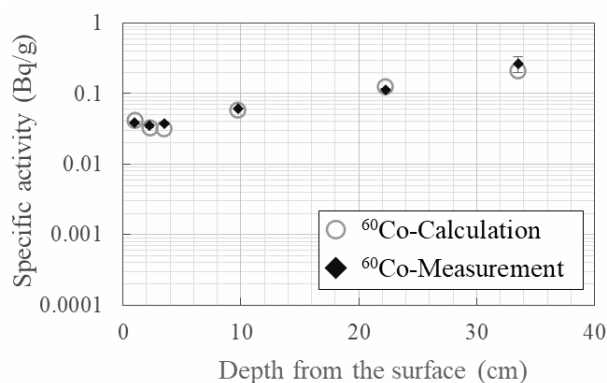


Fig. 1. Depth distribution of ⁶⁰Co activity in the iron yoke of PET-cyclotron at NMCC.

REFERENCES:

- [1] G. Yoshida, H. Matsumura *et al.*, The 3rd JSRM / JHPS Joint Conference (IC5-4), online, 1-3. Dec. 2021.
- [2] G. Yoshida, K. Nishikawa *et al.*, J.Radioanal. Nucl.Chem. **325** (2020) 801-806.

CO12-2 Neutron Resonance Spectrometry for Nuclear Security and Safeguards Education

J. Kawarabayashi, R. Sasaki, R. Watanabe, A. Miura, T. Takeuchi, D. Ibuki and J. Hori¹

Department of nuclear safety engineering, Tokyo City University

¹ KURNS

INTRODUCTION: In order to support nuclear facility regulations in Japan for safe use, it is necessary to develop educational training course with broad knowledge associated with nuclear engineering. Nuclear facilities include reprocessing, nuclear fuel factories, research facilities, etc. in addition to nuclear power plants, it is important to teach not only the knowledge of radiation, reactor physics, but also the physics of nuclear material itself at each stage of the nuclear fuel cycle. The knowledge of physical and chemical properties of nuclear material is also needed for effective regulation. As a part of this human resource development, we have proposed an isotope ratio measurement training program with uranium using pulsed neutron spectrometry as a candidate for the nuclear regulatory educational course to deepen the understanding of the nuclides in nuclear fuel cycle. Observation of the neutron resonance absorption phenomena of natural, enriched and depleted uranium will develop the understanding of the isotope itself and the properties of the nucleus of uranium. In this fiscal year, as the pandemic of Covid-19 limited our student to travel to Kyoto University, we tried to establish an online experiment to acquire neutron resonance absorption spectra of various samples.

EXPERIMENTS: Samples of six different elements (Ag, In, Mn, Co, Cd, U) were irradiated at KURNS-LINAC to record neutron transmission spectrum. A ³He proportional counter followed by a multiple-stop time spectrometer (ORTEC EASY-MCS) was located behind the sample at 13m experimental room and generated timing signal of neutron detection. A signal from the accelerator was used as the start signal of the time spectrometer. The timing calibration between start signal and output signal of the ³He proportional counter was performed with an oscilloscope by gamma-flash signal generated at the Ta target of the accelerator. The sample of Uranium was arranged at in front of the neutron irradiation port and time spectra of neutron transmission were recorded. Five students participated in the experiment over computer network by Zoom meeting software.

RESULTS: As shown in left part of Fig. 1, a resonance dip of ¹⁰⁹Ag was clearly observed in the time spectrum with the sample of silver plate (thickness: 1.0 mm) successfully, with measurement of 60,000 sweeps and 20 msec. range. The accelerometer was running at 50Hz with pulse-width of 4 micro sec. per pulse. The time spectrum was recorded within about 20 minutes. The energy of this dip was estimated to be 5.3 eV derived

from the source-detector distance of 12 m and dip position of 0.377 msec. The first energy level of ¹⁰⁹Ag is 5.19 eV [1]. There is a good agreement between the experimental result and literature value. In right part of Fig. 1, time spectrum with In plate (thickness: 1 mm) were obtained. There were three resonance dips corresponding to ¹¹⁵In. We confirmed the dips corresponded to resonant absorption energies of 1.46 eV, 3.85 eV, 9.07eV[1]. Fig. 2 shows the time spectrum of natural Uranium (left) and enriched Uranium (right, ²³⁵U amount of 0.416 g) samples. We can observe three clear resonant dips corresponding to the first, second and third levels of ²³⁸U nucleus in the left part of Fig. 2. In the observed time spectrum of enriched U, we can see the first resonance wide dip of ²³⁵U around 0.3 eV at TOF of 1.5 msec. and several weak resonance dips at 0.29 msec. and 0.34 msec. The screen of the PC acquiring these spectra was shared with online students through Zoom-meeting software. The online students were able to observe the acquisition of neutron transmission spectra in real time. The experimental system and conditions were explained online with a video taken in the morning of the day when the experiment was carried out. Interviews with students after training showed that the content of the experiment could be understood online.

CONCLUSION: We proposed pulsed neutron spectrometry as a candidate for the nuclear regulatory educational course to deepen the understanding of the nuclides in nuclear fuel cycle and performed online training program. The results showed that online program was able to support for students to understand the difference of the cross-sections of ²³⁵U and ²³⁸U for low energy neutron.

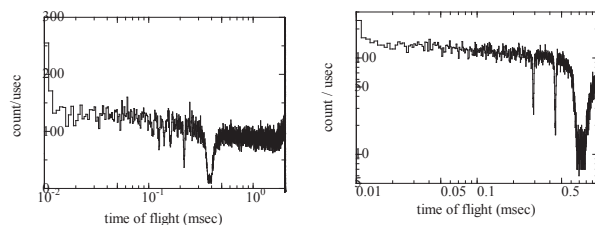


Fig. 1. ToF spectrum of Ag (left) and In (right).

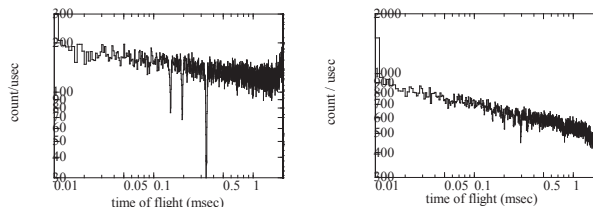


Fig. 2. ToF spectrum of natural U (left) and enriched U (right).

REFERENCES:

[1] S. F. Mughabghab, Atlas of Neutron Resonances.

CO12-3 Structural Analysis of Additives in Lubricants by Small-Angle X-ray Scattering

T. Hirayama, S. Nambo¹, W. Yagi¹, Y. Takashima², N. Sato³ and M. Sugiyama³

Graduate School of Engineering, Kyoto University

¹Graduate School of Engineering, Kyoto University

²Idemitsu Kosan Co., Ltd.

³Institute for Integrated Radiation and Nuclear Science, Kyoto University

INTRODUCTION: Tribology is a research field that deals with friction, wear, and lubrication techniques on mechanical sliding surfaces, and many efforts have been made to reduce friction. In recent years, some researchers have proposed the use of fullerenes (C60) in lubricants to reduce the friction between two surfaces, and their effectiveness has been verified. In fact, several research groups have reported that fullerenes are effective in reducing friction when mixed at relatively high concentrations of 1000 ppm or more, and fullerenes are highly anticipated as a lubricant additive in the near future. However, there are reports that the size of the effect varies depending on the base oil, and it is assumed that the effect depends largely on the dispersion form of fullerenes in the base oil, but the actual state remains unclear. In this study, the dispersion morphology of fullerenes in various base oils are investigated using small-angle X-ray scattering (SAXS).

EXPERIMENTS: SAXS analysis was performed to understand the dispersion morphology of fullerenes in lubricant under various temperature conditions. A SAXS spectrometer with Cu radiation source installed at the Institute for Integrated Radiation and Nuclear Science, Kyoto University, was used for the analysis. First, fullerenes were dissolved in polyalphaolefin (PAO4) at a concentration of 1000 ppm, which was used as the target sample. The temperature conditions were 25°C and 100°C. The radius of gyration R_g of fullerenes in PAO was estimated from the obtained scattering profiles.

RESULTS: The obtained scattering curve is shown in Fig. 1, and its transformation into a Guinier plot is shown in Fig. 2. The radius of gyration of the fullerenes in PAO was found to be 0.78 nm at 25°C and 0.96 nm at 100°C, respectively. No aggregation of fullerenes was observed in PAO. Since the outer diameter of a fullerene is approximately 1.4 nm, the radius of gyration of fullerene in PAO is almost the same as the original size. It remains to be verified whether this is due to the fact that the fullerenes are covered with PAO molecules, but at least it was confirmed that the radius of gyration and the aggregation form of the fullerenes in the base oil can be estimated by SAXS analysis.

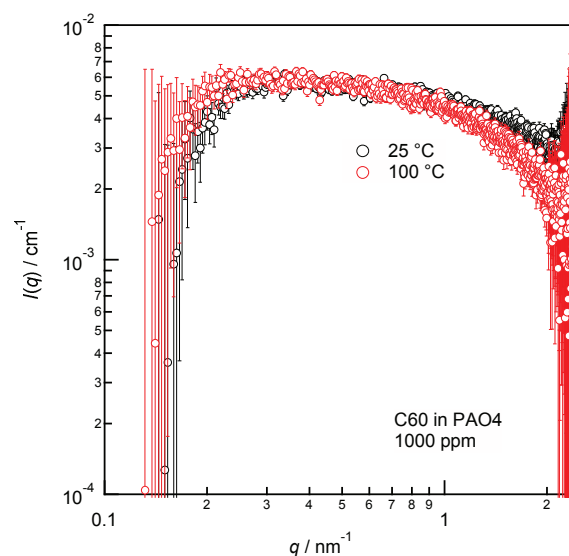


Fig. 1 $I(q)$ profiles of C60 in PAO at 25 and 100°C.

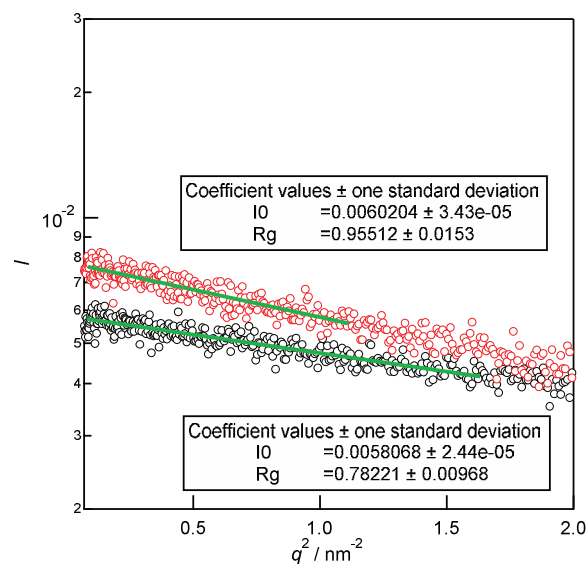


Fig. 2 Guinier plots transformed from Fig. 1.

CO12-4 Visualization of Lubricant Behavior in Machine Elements by Neutron Phase Imaging

T. Hirayama, L. Sun¹, Y. Seki², T. Shinohara³, M. Hino⁴ and R. Nakamura⁴

Graduate School of Engineering, Kyoto University

¹*Graduate School of Engineering, Kyoto University*

²*Institute of Multidisciplinary Research for Advanced Materials, Tohoku University*

³*J-PARC center, Japan Atomic Energy Agency*

⁴*Institute for Integrated Radiation and Nuclear Science, Kyoto University*

INTRODUCTION: Engineering related to friction, wear, and lubrication on mechanical sliding surfaces have been studied intensively in the field of tribology. In particular, the formation of oil film has a great influence on the tribological properties of sliding surfaces, and since the friction coefficient of a sliding surface varies greatly depending on the presence or absence of oil film, it is extremely important to predict the state of lubrication of sliding surfaces. In the field of tribology, the Reynolds equation is generally used to predict the state of oil film formation. However, when the Reynolds equation is applied to sliding bearings, for example, the boundary condition of atmospheric pressure at the end of the sliding bearing is often used. On the other hand, it is difficult to understand the behavior of the gas-liquid boundary at the end of machine elements such as sliding bearings because they are often made of metal and are difficult to visualize.

In this study, we attempted to understand the shape of the gas-liquid boundary at the end of a sliding bearing by using neutron phase imaging. The main reasons for using neutron phase imaging are as follows.

1. The high penetrability of neutron beams enables direct observation of the gas-liquid boundary.
2. The contrast of the area to be observed can be adjusted arbitrarily by deuterating a part of the liquid.

EXPERIMENTS: In this study, we used the cold neutron beamline CN-3 at Institute for Integrated Radiation and Nuclear Science, Kyoto University. Neutron phase imaging is a new visualization technique that uses a Talbot-Lau interferometer to detect the phase change of the neutron beam after it penetrates an object and to obtain an image of the waveform. The visibility image obtained by this method is particularly suitable for this study because it can map the microscopic inhomogeneous state of size and density of molecules in the target field.

A bearing model used in the experiment is shown in Fig. 1, and the tapered shape of the sliding bearing end is also shown in Fig. 1.

RESULTS: The transparent contrast image, differential phase contrast image, and visibility contrast image obtained from the experiment are shown in Fig. 2. In this experiment, polyalphaolefin (PAO), a common machine

oil, was used as the sample oil. It can be said that the numerical calculation of the images obtained by the phase imaging method enabled us to obtain images focusing on the information we expected to obtain.

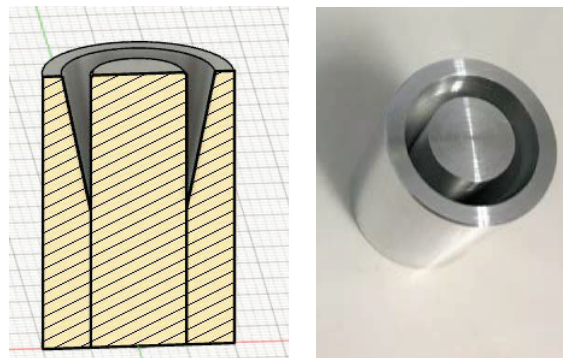


Fig. 1 Sliding bearing model with taper seal at the bearing end made from Aluminum.

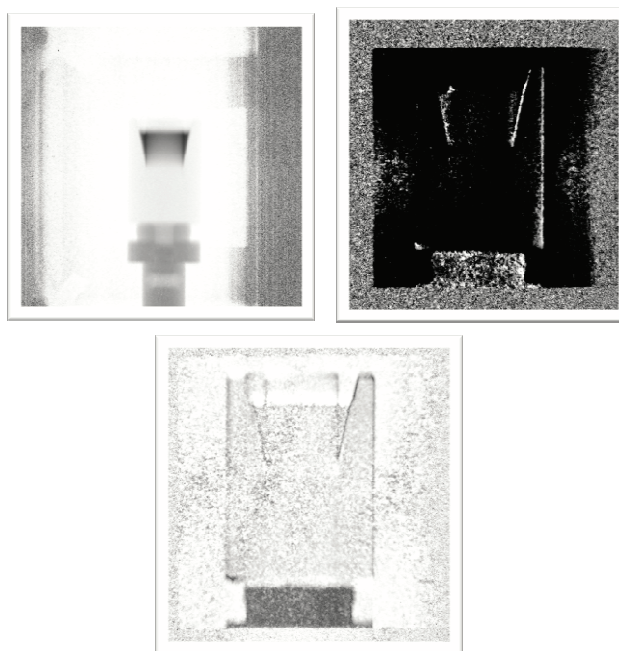


Fig. 2 Obtained images; transparent contrast image (upper left), differential phase contrast image (upper right), and visibility contrast image (lower).

CO12-5 Neutron Activation Analysis of Neodymium Oxide

T. Miura¹, S. Sekimoto², R. Okumura², H. Yoshinaga², Y. Iinuma²

¹National Metrology Institute of Japan, AIST

²Institute for Integrated Radiation and Nuclear Science, Kyoto University

INTRODUCTION: National Metrology Institute of Japan (NMIJ) is responsible for developing certified reference materials and for establishing the traceability of SI (The International System of Units) on chemical metrology in Japan. To establish SI traceability, the primary method of measurements should be applied to the characterization of the certified reference materials. Neutron activation analysis using comparator standard is recognized as a potential primary ratio method [1]. Despite the potential of neutron activation analysis as primary ratio method, the evaluation the measurement capability and the measurement uncertainty are required in any analysis. In general, there are three main components of uncertainty in neutron activation analysis, that is, sample preparation uncertainty, neutron flux homogeneity, and gamma ray measurement uncertainty. Usually, flux monitor is used to correct the neutron flux heterogeneity. However, although the flux monitor can correct the neutron flux variation using the count rate of the known amount of the monitor nuclide, it does not reflect the neutron flux of the actual sample. The most practical method to eliminate neutron flux heterogeneity to improve gamma ray measurement uncertainty is an internal standard method [2, 3]. For the development of primary inorganic standard solution as national standard, the purity of starting material has to be determined. The high purity neodymium oxide was candidate starting material for preparation of Nd standard solution as national standard of Japan. The several trace analytical methods including neutron activation analysis, were used for purity determination of the high purity neodymium oxide. In this work, we presented that capability of instrumental neutron activation analysis for determination of Sc, La, Pr, Sm, Eu, Gd, Tb, Dy, Ho, Er, Yb, and Lu as impurity about rare earth elements in the neodymium oxide.

EXPERIMENTS: The high purity neodymium oxide (Alfa Aesar, Reacton) purchased from FUJIFILM Wako Pure Chemical Corporation. The informative purity value of the neodymium oxide was 99.999 %. NIST SRM single element standard solutions (3148a Sc, 3127a La, 3142a Pr, 3147a Sm, 3117a Eu, 3118a Gd, 3157a Tb, 3115a Dy, 3123a Ho, 3116a Er, 3160a Tm, 3166a Yb, 3130a Lu) were used for calibration standard in impurity analysis of the neodymium oxide, respectively. The standard solutions were added on filter paper to prepare the calibration standard in the analysis. The prepared calibration standards were heat sealed into polyethylene bags. Ten mg of the neodymium oxide samples were used for impurity analysis. The neutron irradiations performed

by KUR Pn2 (thermal neutron flux: $5.5 \times 10^{12} \text{ cm}^{-2}\text{s}^{-1}$) for 5 min, Pn3 (thermal neutron flux: $4.7 \times 10^{12} \text{ cm}^{-2}\text{s}^{-1}$) for 1 min and TcPn (thermal neutron flux: $8.0 \times 10^{10} \text{ cm}^{-2}\text{s}^{-1}$) for 12 h. The irradiated samples were cooled appropriately. The gamma rays from irradiated samples were measured using Canberra GC4070-7500 Ge detector with Laboratory Equipment Corporation MCA 600. The measure radioactive isotopes were ⁴⁶Sc, ¹⁴⁰La, ¹⁴¹Ce, ¹⁴²Pr, ¹⁵³Sm, ^{152m}Eu, ¹⁵⁹Gd, ¹⁶⁰Tb, ¹⁶⁵Dy, ¹⁶⁶Ho, ¹⁷¹Er, ¹⁷⁰Tm, ¹⁷⁵Yb and ¹⁷⁷Lu.

RESULTS: Analytical results of the high purity neodymium oxide were shown in Table 1. In this measurement, Sc, Pr, Sm, Eu, Gd, Tb, Dy, Ho, Er, Yb, and Lu in the neodymium sample could not be detected by instrumental neutron activation analysis. Therefore, the detection limits for these elements were estimate from the count rate of energy region of gamma rays emitted by induced radioactive nuclides. The estimated detection limits were also presented on Table 1.

Table 1. Analytical results of the high purity neodymium oxide

	Measured values, mg/kg
Sc	< 0.3
La	0.4 ± 0.16
Pr	< 4
Sm	< 1
Eu	< 0.04
Gd	< 40
Tb	< 8
Dy	< 0.7
Ho	< 4
Er	< 11
Yb	< 6
Lu	< 2

REFERENCES:

- [1] R. Greenberg, P. Bode, E. De Nardi Fernandes (2011) Spectrochim. Acta B, 66, 193-241.
- [2] T. Miura, K. Chiba, T. Kuroiwa, T. Narukawa, A. Hioki, H. Matsue (2010) Talanta, 82, 1143-1148.
- [3] T. Miura, R. Okumura, Y. Iinuma, S. Sekimoto, K. Takamiya, M. Ohata (2015) J. Radioanal. Nucl. Chem., 303, 1417-1420.
- [4] NuDat 2, National Nuclear Data Center in Brookhaven National Laboratory, <https://www.nndc.bnl.gov/nudat2/index.jsp>.

CO12-6 Observation of Superposition of Coherent Transition Radiation Using an Extra Ring Resonator

N. Sei, and T. Takahashi¹

Research Institute for Measurement and Analytical Instrumentation, National Institute of Advanced Industrial Science and Technology

¹Institute for Integrated Radiation and Nuclear Science, Kyoto University

INTRODUCTION: A coherent radiation generated by a relativistic electron beam, which was observed for the first time in Japan [1], becomes high power in the terahertz-wave region. Therefore, many light sources using the coherent radiation have been developed at various electron linac facilities. Using an L-band linac at Kyoto University Institute for Integrated Radiation and Nuclear Science (KURNS-LINAC) [2], we have also demonstrated a new radiation principle that is superior to coherent transition radiation (CTR) in radiation power [3]. However, the development of the new radiation principle is not the only effective means to obtain intense terahertz waves. By matching phases of multiple terahertz-wave sources, higher power terahertz waves can be obtained [4]. Then, we proposed that coherent radiation generated by a pulse train of electron bunches was confined in a ring resonator and superimposed with the same phase. In the initial experiments, it was confirmed that a CTR beam was amplified by using a ring-type optical cavity installed in the electron beam orbit. However, it was difficult to adjust a cavity length of the optical cavity because it was installed in a vacuum chamber. Therefore, in order to adjust the cavity length, the optical cavity was set in the experimental room to guide the CTR beam into it. An amplification depending on the cavity length was successfully observed.

EXPERIMENTS: The CTR beam extracted from the coherent radiation beamline to the atmosphere in the experimental room was adjusted to a parallel beam with a diameter of 42 mm using two concave mirrors. It was guided to a Cyclo Olefin Polymer (COP) substrate with a thickness of 3 mm in the ring-type optical cavity, and a part of the CTR beam reflected on the surface of the COP substrate accumulated in the optical cavity. The optical cavity consisted of two parabolic mirrors with a focal length of 508 mm and two plane mirrors, and the cavity length was 922 mm, which corresponded to four electron micropulse intervals. The COP had a refractive index of 1.531 and its absorption coefficient was negligible in the terahertz-wave region [5]. Approximately 8% of the CTR beam accumulated in the optical cavity was emitted to the outside of the optical cavity by reflection from both sides of the COP substrate per circumference of the optical cavity. The emitted CTR beam was synchronized with the CTR beam transmitted through the COP substrate without entering the optical cavity. These CTR beams were focused by a parabolic mirror with a focal length of 101

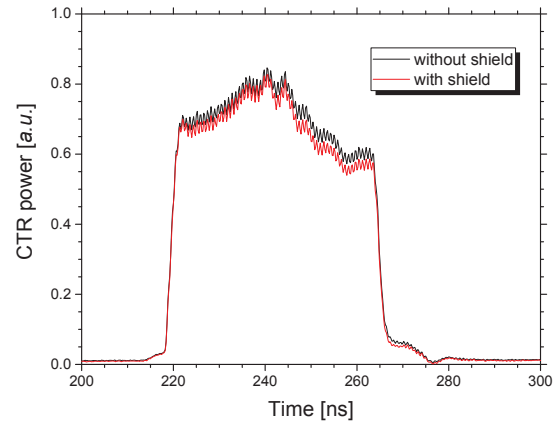


Fig. 1 Measured CTR power emitted from the optical cavity with (red line) and without (black line) an absorber in the optical cavity.

mm and detected by a D-band diode detector (Millitech Inc., DXP-06) with an antenna [6]. The output signal of the diode detector was measured by an oscilloscope with the frequency band less than 350 MHz.

RESULTS: We conducted experiments using the KURNS-LINAC electron beam with the electron energy of 41 MeV and the current of 2.4 μ A. The duration of the electron-beam macropulse was set to be 47 ns. Figure 1 shows the measured powers of the CTR beams emitted from the optical cavity with and without an absorber in the optical cavity. The difference between two lines in this figure represents the presence of the CTR beam accumulated in the optical cavity. It is noted that the resonated CTR beam increased with the time in the macropulse. Because the power of the resonated CTR beam depended on the cavity length, it is considered that the CTR power was amplified by superimposing the each CTR pulse orbiting the ring-type optical cavity.

In the next experiment, we plan to install the optical cavity in the electron beam orbit to clarify the relationship between the cavity length and the amplification of the CTR power.

REFERENCES:

- [1] T. Nakazato *et al.*, Phys. Rev. Lett., **63** (1989) 1245-1248.
- [2] T. Takahashi and K. Takami, Infrared Phys. Technol., **51** (2008) 363-366.
- [3] N. Sei and T. Takahashi, Sci. Rep. **7** (2017) 17440.
- [4] N. Sei and T. Takahashi, Sci. Rep. **10** (2020) 7526.
- [5] http://www.tydexoptics.com/pdf/THz_Materials.pdf.
- [6] N. Sei *et al.*, J. Phys. D: Appl. Phys. **46** (2013) 045104.

CO12-7 Another Trial to Analyze the Texture of Roof-tile: Toward Detailed Provenancial Studies of Excavated Ceramics by INAA

M. Tomii, K. Takamiya¹, H. Yoshii, M. Kidachi², A. Ito, and Y. Chiba

Graduate School of Letters, Kyoto University

¹Institute for Integrated Radiation and Nuclear Science, Kyoto University

²College of Letters, Ritsumeikan University

INTRODUCTION: Following the last year trial, in order to establish the procedures to archaeologically identify local groups for production of ceramics in Japan, 16 pieces of the roof-tiles with stamp impression from the same collection as the one in last year are analyzed. They were excavated from the archaeological site in Kyoto in 1992, where the garrison from the *Tosa* domain had occupied in the mid-19th century. The normal type of roof-tiles in the collection is almost exclusively composed of the ones having the stamp impressions of Chinese characters which indicate the name of maker/atelier of the tile. 24 kinds of stamp impression have been recognized in this collection, and 23 stamp impression groups of the 24 suggest the makers in *Tosa* region at that time [1].

Despite the difference in potter's names written in the impressions, it has been improbable to divide pieces in the whole collection into groups in terms of size and production technique. This study thus tries to check whether the groups based on the difference in stamp impressions, suggesting different production groups, corresponds with the groups of tile texture in detail.

EXPERIMENTS: Conventional INAA was applied to determine the elemental composition of samples of the tiles, each of which had been drilled into a fine powder as a sample by Maria Shinoto (Universität Heidelberg), and the same was also done by Johannes Sterba (Technische Universität Wien) at the Atominstitut in Wien (Vienna) for comparison [2]. In KURNS, 16 pieces of the roof-tile of normal type, composed of three stamp impression groups, were chosen; seven were from the "AKIBUN" group, another seven from "AKIKANE" group, and the rest two, each of which had two samples for double measurement, respectively, from "SUMIKAWARA" group. Each 18 samples, enclosed in a polyethylene bag, was neutron-irradiated, firstly at Pn-3 of KUR (1 MW) for 90 seconds to detect short-lived nuclides, and then at Hyd (1MW for 23 hours and successively 5 MW for 6 hours) to determine long-lived nuclides. The comparative standards (JR-3, JB-1b) were irradiated with the same condition. Around 20 mg was used for Pn-3 and around 30 mg for Hyd, in each sample.

The gamma-ray spectrometry of the irradiated samples for short-lived nuclides had been performed four times based on the last year experience; just after the irradiation, after 15 minutes, 40 minutes, and around 20 hours. The photo-peak analysis for short-lived nuclides was performed by using FitzPeaks [3]. Concentrations of elements

included in the samples were estimated by comparison of the intensity of gamma-rays between the comparative standard and tile samples.

RESULTS: Concentrations of nine elements (Na, Mg, Al, K, Mn, Ga, La, Sm and Th) in every sample were determined. Samples irradiation by Hyd for determination of long-lived nuclides could not be recovered because of adhesion of plastic bags for sample sealing during irradiation. Before the comparison with the result in Atominstitut, which analyzed exactly the same roof-tiles, estimation of the elemental concentrations for long-lived nuclides is inevitably required at KURNS to apply the Mahalanobis Distance for quantitative investigation into the 16 tiles. Nevertheless the following two results can be pointed out;

- a) both two sets for double measurement suggest that two elements (Al and Mg) have a wider range of value of concentration (table 1).

Table 1 Concentration ($\mu\text{g/g}$) of two elements determined for the roof-tiles "KS92-466" and "KS92-693".

Tile	Al	Mg
KS92	4.36E+04 \pm 8.94E+02	5.27E+02 \pm 1.21E+02
-466	5.73E+04 \pm 1.09E+03	7.06E+02 \pm 1.58E+02
KS92	6.79E+04 \pm 1.30E+03	7.97E+02 \pm 1.77E+02
-693	5.65E+04 \pm 1.12E+03	6.59E+02 \pm 1.47E+02

- b) two elements (Na and Mn) show a clear difference in concentration to divide 18 samples into two groups, respectively, and the concentrations combination of the two suggests the three groups, which fully correspond with the stamp groups (Fig.1).

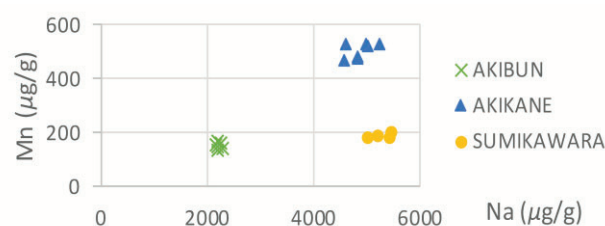


Fig 1 Distribution of 18 samples on the concentrations combination of Na with Mn.

ACKNOWLEDGEMENT

We would like to thank Dr Johannes Sterba and Dr Maria Shinoto for performing the sampling procedures on the sherds according to the workflow established in Vienna.

REFERENCES:

- [1] Y. Chiba *et al.*, *Annual Report of Archaeological Researches in KU sites for 1992*. (1995) 65-125.
- [2] J. Sterba, *J. Radio. Nucl. Chem.*, **316** (2018) 753-759
- [3] J. Fitzgerald, FitzPeaks Gamma Analysis and Calibration Software, <https://www.jimfitz.co.uk/fitzpeak.htm>

CO12-8 Development of high-count rate two-dimensional neutron detector system

S. Sato, K. Mori¹, Y. Yoshino¹, T. Seya, T. Otomo, H. Oshita

High Energy Accelerator Laboratory, KEK
¹ Institute for Integrated Radiation and Nuclear Science,
Kyoto University

INTRODUCTION: Most of the neutron detectors currently in use are ³He gas detectors, and some neutron scintillator detectors are used to obtain a high counting rate and high position resolution. In this study, the LiTA system [1] has been developed as a high counting rate two-dimensional detector system. However, it is expensive and difficult to use, and it has been not widely used. Therefore, we have developed an ADCnet64 system at last year as a low-cost, simple using, and high-counting-rate two-dimensional neutron detector system instead of the LiTA system. The performance of the ADC net64 system had been evaluated using the B3 port of KUR continuously.

EXPERIMENTS: The ADCnet64 system is a readout circuit for high-speed scintillators. It has 64-channel high-speed analog to digital converters (ADCs) with 10 bits 80 MHz sampling rate to read a 5 cm square 8 × 8 multi-anode type photomultiplier tube. Although the ADCnet64 system is inferior to the LiTA system in performance, similar data are obtained with fewer circuits and easy way.

This year, we used a 1 mm thickness of ⁶Li and explored ways to achieve better position resolution and higher detection efficiency with the B3 port.

Since the ADCnet64 system uses a photo-multiplier tube with 64 anodes spaced 6 mm apart, it was found that a single threshold value did not give good characteristics. Figure 1 shows the single threshold data, which has good position resolution but poor detection efficiency. It is only 57 % more efficient than Figure 2. Figure 2 shows the data with a low hardware threshold and a high software threshold, which proved to have both good position resolution and detection efficiency.

RESULTS: We have developed the ADCnet64 system with a low-cost, simple, high-counting-rate, and two-dimensional neutron detector. We have evaluated its performance using the B3 port at KUR.

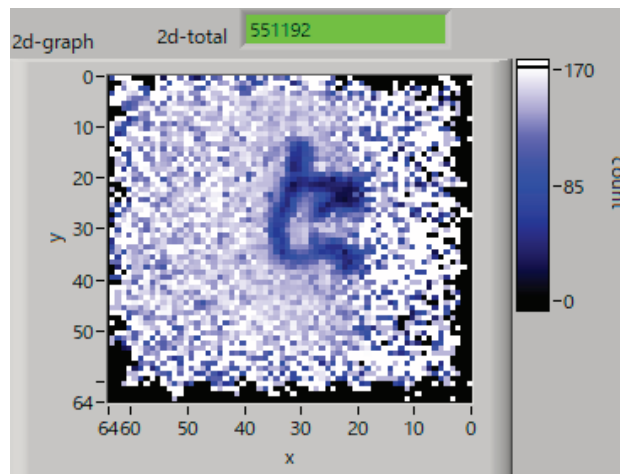


Fig. 1. Two-dimensional graph using ⁶Li glass in 1 mm thickness by the single threshold.

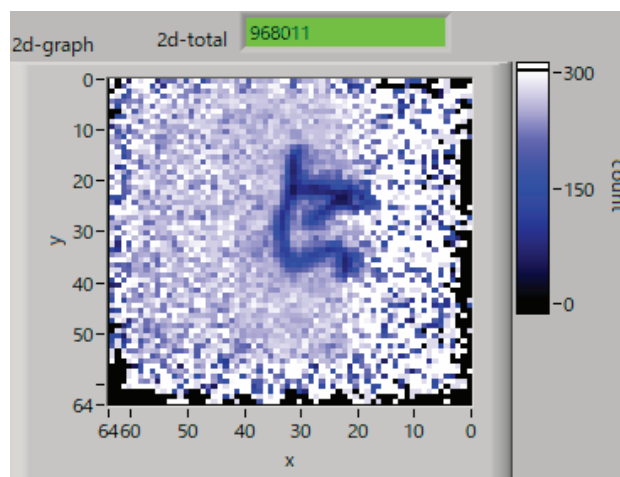


Fig. 2. Two-dimensional graph using ⁶Li glass in 1 mm thickness by the two thresholds.

REFERENCES:

- [1] S. Satoh, UCANS-V 2015, DOI 10.1393/ncc/i2015-15197-7.

CO12-9 Study for activity measurement technique of radioactive noble gases using a plastic scintillator

Takahiro Yamada^{1,3}, Tatsuya Yamada², Ken-ich Mori³ and Hiroshi Yashima⁴

Kindai University

¹Atomic Energy Research Institute

²Faculty of Science and Engineering

³Graduate school of Science and Engineering

⁴Institute for Integrated Radiation and Nuclear Science, Kyoto University

INTRODUCTION: In order to calibrate monitors used for measuring radioactive noble gases in nuclear power plants or reprocessing facilities, use of activity reference measurement standard gases shall be required. A β -ray counting technique using a set of multiple ventilated proportional counters having different lengths is generally used to determine activity concentration of standard gases [1]. In this study, a method based on the $4\pi\beta\text{-}\gamma$ spectroscopic method using a plastic scintillator (PS) as a β -detector was carried out to measure activity of ^{41}Ar absolutely as an alternative approach.

EXPERIMENTS: ^{41}Ar gas was produced via $^{40}\text{Ar}(n,\gamma)^{41}\text{Ar}$ reaction. Pure argon gas was filled into the small crystal glass container having 10 ml with atmospheric pressure and was irradiated for 60 s at the bottom of KUR-SLY under operating at 1 MW thermal output. Around 300 kBq of ^{41}Ar was produced with $7.84 \times 10^{11} \text{ n}^{-1}\text{s}^{-1}\text{cm}^{-2}$ of the nominal flux of the thermal neutron. The radioactive gas was transferred to a large volume container and diluted with stable argon gas. In the present study 5 kBq of ^{41}Ar produced at UTR-KINKI was also used without dilution.

A small acrylic gas container with internal dimensions of $\phi 60 \text{ mm} \times 40 \text{ mm}$ (113 ml) was used as the β -detection part of the measurement system. The entire inner wall of the container was lined with 1 mm thick of PS. In addition, to observe β -spectra from each PS set on three different positions (top, bottom and side) of the inner wall separately, a series of measurements using a gas container lined with 1 mm PS on the top, bottom or side was also carried out. The container was covered with aluminum tape on the sides and white tape on the top as a reflector, and a photomultiplier tube (PMT) was connected to the top of the container and stored in a light-shielded case. The β -detector was placed directly onto the Ge detector, and the signal outputs from the β - and γ -detectors were fed to the signal inputs of a multi-channel analyzer (MCA) capable of acquiring data in list mode to obtain list data consisting of the pulse height from each detector and a time stamp of the detection time. ^{41}Ar emits γ -ray ($E_\gamma=1293 \text{ keV}$) following disintegration by beta minus decay to excited levels of ^{41}K with branching ratio of 0.9917 [2]. In order to obtain the β - γ coincidence spectrum from the time-stamped pulse height data, the γ - signals derived within $4.5\mu\text{s}$ from the β -detection time stamps were considered as true coinci-

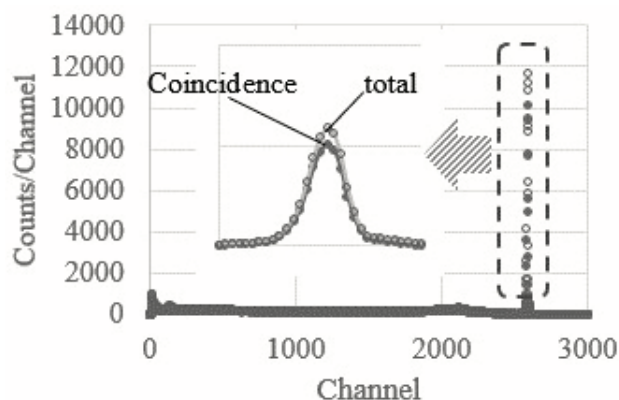


Fig. 1. Coincidence- and γ -spectra obtained from the present measurement using ^{41}Ar .

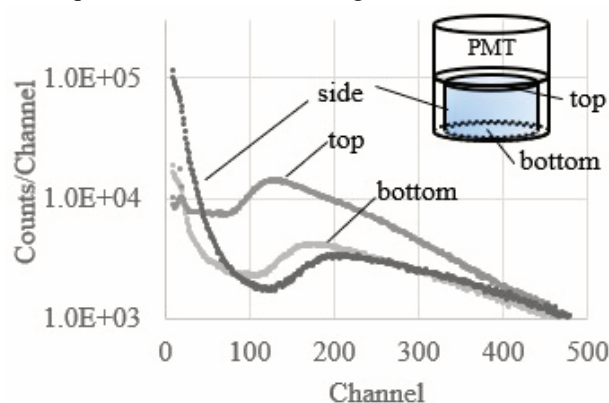


Fig. 2. β -spectra observed by a set of measurements using a gas container lined with 1 mm PS on the top, bottom or side.

dences. β -counting efficiency ε_β is determined as the ratio of net peak area in the coincidence spectrum n_c to the net peak area n_γ in the γ -spectrum.

RESULTS: Figure 1 shows the coincidence and γ -ray spectra obtained in the present experiment. β -counting efficiency determined as n_c / n_γ was 0.872 ± 0.001 . The β -spectra observed by a set of measurements using a gas container lined with 1 mm PS on the top, bottom or side were shown in Fig. 2. As shown in this figure, the spectra obtained from the PS on the side or the bottom were significantly degraded as compare with a spectrum obtained from the PS on the top, where is closest to the PMT, indicating that the difference in light collection at each position of scintillator was considered to be one of the reasons for the counting efficiency decrease of more than 10 %.

REFERENCES:

- [1] A. Yunoki, T. Yamada and H. Yashima, KURNS Progress Report 2019, ISSN 2434-9488, CO12-5 (31059).
- [2] Bé, M., 2011. Table of Radionuclides. http://www.nucleide.org/DDEP_WG/DDEPdata.htm

CO12-10 Fiber-reading Radiation Monitoring System with an Optical Fiber and Red-emitting Scintillator at the ^{60}Co Radiation Facility II

S. Kurosawa^{1,2}, C. Fujiwara², A. Yamaji^{1,2}, H. Tanaka³

¹New Industry Creation Hatchery Center, Tohoku University

²Institute for Materials Research Tohoku University

³Institute for Integrated Radiation and Nuclear Science, Kyoto University

INTRODUCTION: Decommissioning reactors at the nuclear power plant with safety is an important issue in Japan, and a real-time dose-rate monitor in the extremely high radiation dose condition is required for the above application.

Cs_2HfI_6 (CHI) has a high light output (over 60,000 photons/MeV), high effective-atomic number (over 60), red and infrared emission (600 – 800 nm) and no after-glow (less than 1% within 1s), and this material is available for such dose monitors. On the other hand, this material cannot be applied to alpha-ray detection due to the package for the hygroscopic nature[1,2].

Since the size of the scintillation sample should be small as well as a few mm^3 due to the fiber diameter and space limitation in the power plant, a high effective gamma-ray efficiency and no package against the hygroscopic nature are required. One of the candidate materials is Yb-doped $\text{La}_2\text{Hf}_2\text{O}_7$ (Yb:LHO), because this atomic number is 64. Moreover, Yb-doped samples are expected to have an infrared sharp peak around 970 nm originating from Yb^{3+} of 4f-4f transition. Although Yb:LHO has a high melting point of over 2400°C, we grew this crystal by the Core-Heating (CH) method, which we have developed as a novel crystal-growth technique in 2020[3].

Last year, we reported the intensity of Yb:LHO has lower intensity (1% of CHI) than those of $\text{Cr}:\alpha\text{-Al}_2\text{O}_3$ (10% of CHI), and the dose-rate dynamic range was narrow than the others. In this year, we evaluated the signal-noise-to ratio, precisely.

EXPERIMENTS: We fabricated a Yb:LHO sample grown by the CH method, and the demonstration was performed at the ^{60}Co Gamma-ray Irradiation Facility with an activity of ~ 70 TBq. The monitor and setup were the same as that last year; and an optical fiber (S.600/600B, Fujikura) had a length of 20 m and a pure SiO_2 with a core diameter of $600 \pm 30\mu\text{m}$. The scintillation light was transmitted through the fiber and measured with a CCD spectrometer (Blue-UVNb, StellarNet). We defined the signal-to-noise ratio as shown in Fig. 1; The integral range was over 10% peak value in the wavelength region as signal and noise.

RESULTS: We succeeded in growing the transparent Yb:LHO sample, and the sample and fiber were assembled. The assembly was irradiated with gamma rays from the ^{60}Co source, and the emission spectrum was obtained as

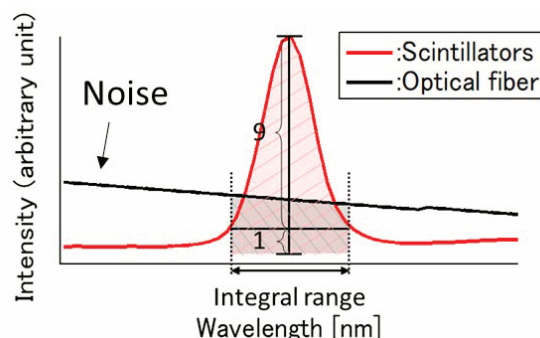


Fig. 1 Definition of integrating zone.

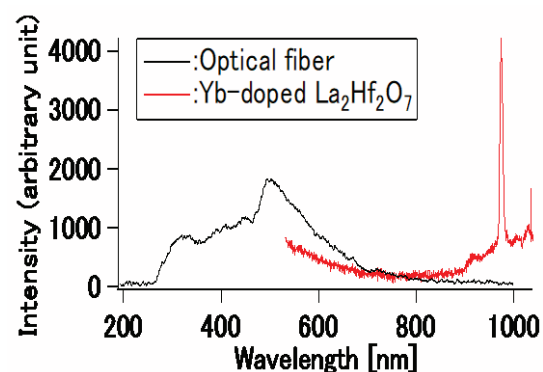


Fig. 2 Emission spectra of Yb:LHO+optical fiber and only fiber irradiated with gamma rays from the ^{60}Co source

shown in Fig.2. Here, this spectrum included optical fiber noise, and sharp peaks around 974 nm was originating from Yb^{3+} 4f-4f transition.

Moreover, the fiber was also irradiated without Yb:LHO to measure background noise (Fig. 2), and signal-to-noise ratio was calculated. When the scintillator and optical fiber were under 0.18 and 0.87 kSv/h, for instance, the ratio was evaluated to be 0.63 ± 0.2 . On the other hand, CHI has that of 0.55 ± 0.2 . Although Yb:LHO had smaller emission intensity than that of CHI, Yb:LHO had the good ratio compared to CHI due to longer emission wavelength.

As future works, we developed novel scintillators with high emission intensity at 800 – 1000 nm, which is the region of low background level.

REFERENCES:

- [1] S. Kodama *et al.*, Appl. Phys. Express, **13** (2020) 047002.
- [2] S. Kodama *et al.*, Radiat. Meas., **124**, (2019) 54.
- [3] <https://www.tohoku.ac.jp/japanese/2021/01/press20210122-01-core.html>

CO12-11 Size Measurement of Radioactive Aerosol Particles Using a Diffusion Battery and Imaging Plates in an Electron LINAC Facility

Y. Oki, K. Takamiya, M. Inagaki, S. Sekimoto

*Institute for Integrated Radiation and Nuclear Science,
Kyoto University*

INTRODUCTION: Recently mA-class accelerators have been developed for isotope production and medical use. Target melting accidents, such as the J-PARC accident in 2013, could happen easily by mis-handling of high-intensity beam. The nature of radioactive species in air of the accelerator rooms is very important information to estimate behavior of radionuclides emitted from the accidents in addition to ordinary radiation safety control.

During machine operation the accelerator room is filled with radiation-induced aerosol particles in the size range of several nm to ca. 100 nm in addition to radioactive gases. The size for the radioactive particles was often measured using a wire screen technique in accelerator facilities. Convenient size measurement techniques are needed for radiation protection in accelerator facilities. A combination technique with imaging plate (IP) was employed in a proton accelerator facility [1].

In this work, continuing from FY2020, an attempt was made to measure the size of ^{13}N -bearing aerosol particles using the combination technique of screen-type diffusion battery (SDB) and IPs in an electron linear accelerator facility. Nitrogen-13 is a principal radionuclide ($T_{1/2} = 9.965$ min) produced in air of accelerator rooms in electron LINACs.

EXPERIMENTS:

Measurement method: The SDB employed in this work consists of 40 pieces of 500-mesh stainless steel wire screen and a backup filter (PTFE membrane filter). After collection of the aerosol particles with the SDB, selected screens and the backup filter were measured with an IP.

Principle of SDB: When very fine aerosol particles pass through a stack of wire screens, a part of the particles is deposited on the wire surface of the screens by their diffusion according to their particle size. The loss by the screens is expressed as a function of particle size, coarseness and number of screens, and flow rate of particles. The radioactivity-based size distribution of the aerosol particles can be calculated by measuring the penetration ratio (A/A_0), where A_0 and A are activity of the nuclide of the aerosol particles before and after penetrating screens, respectively.

Formation and collection of radiation-induced aerosols: Aerosol-free air was irradiated with an electron beam air-irradiation experiment was carried out in the 46-MeV electron LINAC of the Institute for Integrated Radiation and Nuclear Science, Kyoto University (KURNS). An

irradiation chamber was placed at a rear position of a platinum target in the target room. During the irradiation, aerosol-free air was introduced to the chamber from the experiment room next to the target room. The target was bombarded with a 30-MeV electron beam to produce bremsstrahlung. The bremsstrahlung ionizes air and produces the radiation-induced aerosol. The beam current was ca. 100 μA . The irradiated air was sampled with the SDB at the measurement station in the experiment room.

Estimation of size distribution of radioactive aerosol particles: The IP image of the selected screens and the backup filter was simultaneously taken using a single large IP (Size: 43 x 35 cm). The penetration ratio for the i -th screen was calculated by the dividing total activity of the screens downstream of the i -th screen and the backup filter by the total activity of all screens and the backup filter. In this calculation, the activity of each 500-mesh screen was estimated by fitting of the intensity of photostimulated luminescence (PSL) of the measured 500-mesh screens.

RESULTS AND DISCUSSION: During the sampling the number-based particle size distribution was repeatedly measured using an SMPS (Scanning Mobility Particle Sizer). It was confirmed that the number-based particle size showed a stable lognormal distribution. The curve of the penetration ratios was successfully fitted to a theoretical function [2] for lognormal distributions to obtain the geometric mean and geometric standard deviation of particle diameter.

The preliminary result of the size was found to be in the range of 40 to 60 nm in diameter, which coincided with the particle size previously reported by another SDB method [3]. The activity-based particle size was always larger than the number-based particle size. The radioactive aerosol particles (the radionuclide-bearing radiation-induced aerosol particle) are formed by incorporating a radionuclide atom into the radiation-induced non-radioactive aerosol particle. The activity-based particle size can be simply compared with the number-based size without any correction. Because the number concentration of radiation-induced aerosol particles is several orders of magnitude greater than the activity concentration of radionuclides formed in accelerator air, the possibility of incorporation of plural radioactive atoms into a single the non-radioactive particle is negligible.

REFERENCES:

- [1] Y. Oki *et al.*, J. Radiat. Prot. Res., **41** (2016) 216-221.
- [2] Y.S. Cheng and H.C. Yeh, J. Aerosol Sci., **11** (1980) 313-320.
- [3] Y. Oki, KURNS Prog. Rep., (2019) CO10-7.

CO12-12 Study of Isotope Separation via Chemical Exchange Reaction

R. Hazama, T. Yoshimoto, A. Rittirong, Y. Sakuma¹, T. Fujii², T. Fukutani³, Y. Shibahara³, A. Sunaga³

Graduate School of Human Environment, Osaka Sangyo University

¹Laboratory for Advanced Nuclear Energy, Tokyo Institute of Technology,

²Graduate School of Engineering, Osaka University

³Institute for Integrated Radiation and Nuclear Science, Kyoto University

INTRODUCTION: Chemical isotope separation for calcium and lithium has been studied by liquid-liquid extraction (LLE) with DC18C6 crown-ether [1, 2]. This report describes the change of separation factor (α) for the total of six times multistage process of LLE in terms of different solvent of water and 12M HCl.

EXPERIMENTS: Chemical Isotopic exchange occurs according to the following chemical exchange reaction:
 $^{40}\text{Ca}^{2+}_{(\text{aq})} + ^{48}\text{CaL}^{2+}_{(\text{org})} \rightarrow ^{48}\text{Ca}^{2+}_{(\text{aq})} + ^{40}\text{CaL}^{2+}_{(\text{org})}$ (1)
 , where L represents macrocyclic polyether(18-crown-6). Calcium chloride solution (30% w/w CaCl_2 (aq), and CaCl_2 (12M HCl)) was mixed in an Erlenmeyer flask with 0.07M DC18C6 in chloroform, by the volume ratio of 5/100 mL (aq/org), for 1 minute. The mixture solution was put in the separating funnel for 10 minutes before separation. The loaded solvent was removed with 10 mL pure water for back-extraction.

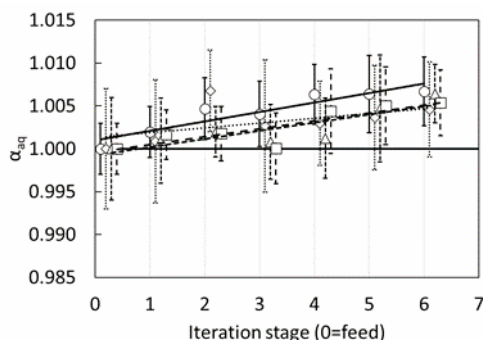


Fig 1. The separation factor (α) of Ca isotope over the iteration stage with 12M HCl acid solvent: Preliminary.

$\bigcirc = ^{48}\text{Ca}/^{40}\text{Ca}$ (—), $\diamond = ^{48}\text{Ca}/^{42}\text{Ca}$ (···),
 $\triangle = ^{48}\text{Ca}/^{43}\text{Ca}$ (-----), $\square = ^{48}\text{Ca}/^{44}\text{Ca}$ (- - -)

The same procedure was iterated using the recovered solution from the previous extraction for six iterations by the new 100 mL organic phase. The calcium concentration was measured by AAS (Shimadzu AA-6800). The isotopic composition was measured by reaction-cell ICP-MS (Agilent 7900: H_2 gas) (Fig 1, 2). It is noted that

our measured isotope ratios of reaction-cell ICP-MS were checked to give the same magnitude by the measurement of TIMS (TRITON and MAT261) by the help of TIT [3].

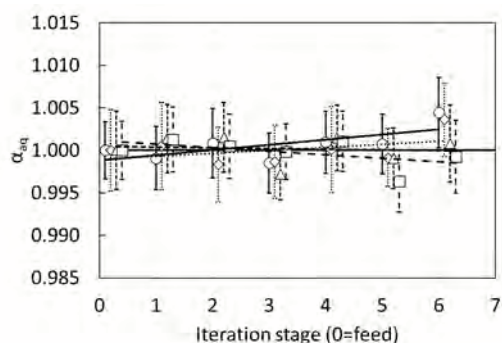


Fig 2. The separation factor (α) of Ca isotope over the iteration stage with aqueous solvent: Preliminary.

$\bigcirc = ^{48}\text{Ca}/^{40}\text{Ca}$ (—), $\diamond = ^{48}\text{Ca}/^{42}\text{Ca}$ (···),
 $\triangle = ^{48}\text{Ca}/^{43}\text{Ca}$ (-----), $\square = ^{48}\text{Ca}/^{44}\text{Ca}$ (- - -)

RESULTS: Multistage iteration using HCl solvent increased the calcium absorption to the crown-ether [2]. Therefore, the recovery of calcium is lower than the aqueous solvent (25.6% and 50.4% for HCl and aqueous solvent at the sixth iteration, respectively). The separation factor (α) ($^{48}\text{Ca}/^{40}\text{Ca}$) of the recovered calcium was 1.007 ± 0.004 and 1.004 ± 0.004 for HCl solvent and an aqueous solvent, respectively (Fig 1, 2). This finding indicated the enrichment feasibility of ^{48}Ca via liquid-liquid extraction under the presence of HCl acid, which can be compared with the chromatographic method [4]. It is noted that the recovery of cation content significantly influences a scale-up on mass production progress of isotope enrichment. Regardless of the calcium recovery, the required iteration to achieve ten-time enrichment of ^{48}Ca was 2112 and 3793 for HCl solvent and an aqueous solvent, respectively. The result shows that the mass production of calcium enrichment is possible via isotope exchange using crown-ether. Moreover, the LLE could be applied to other lighter elements, such as lithium [1, 2, 3], which is widely used in a nuclear reactor.

REFERENCES:

- [1] R. Hazama *et al.*, KURRI Progress Report 2020, 227.
- [2] A. Rittirong *et al.*, J. Phys.: Conf. Ser. 2022, 2147, 012015.
- [3] A. Rittirong, Doctor Thesis, OSU (2022).
- [4] S. Nemoto *et al.*, Journal of Nuclear Science and Technology 2012, 49.4: 425.

CO12-13 Beam Test of a Micro-Cell MWPC for a Muon-Electron Conversion Search Experiment, DeeMe

M. Aoki, N. Abe¹, K. Hase², Y. Higashino, H. Natori³,
Y. Seiya², K. Sugita, T. Takahashi¹, N. Teshima²,
T. Uematsu², and K. Yamamoto²

School of Science, Osaka University

¹*KURNS*

²*Faculty of Science, Osaka City University*

³*Institute of Materials Structure Science, KEK*

INTRODUCTION: The charged-lepton flavor violation (CLFV) process such as the muon-electron conversion has never been observed for unknown reasons. Based on this fact, the charged-lepton flavor is assumed to be conserved a priori in the Standard Model of particle physics (SM). However, it is rather natural to introduce the CLFV processes in the frameworks of many models beyond SM (BSM). Any discoveries or improvements of upper limits on the rate of CLFV processes provide very important information to elucidate BSM. DeeMe is one of experiments to search for the μ -e conversion in nuclear field [1]. It uses high-power high-purity pulsed proton beam from J-PARC RCS and the detector of DeeMe should be operational after an order of micro second from a burst of prompt particles (100 GHz/mm²). We successfully developed a multi-wire proportional-chamber (MWPC) with such a novel feature by introducing high-voltage switching technique [2] and have been performing various R&D for further improvements of overall spectrometer performance.

EXPERIMENTS: The MWPC performance with gas mixtures of Ar : i-C₄H₁₀ (isobutane) : C₃H₈O₂ (methylal) was tested. Addition of methylal is expected to reduce delayed false MWPC-pulses observed for longer than 10 μ s after irradiation of burst electrons (10⁷ electrons/200-ns). Since methylal comes in a liquid state, it must be evaporated to gas by a precisely controlled manner. Such a gas mixture system is rather complicated and we were able to run the system stably after some struggles.

MWPC output-signal gains were measured using low-rate DC electrons from the LINAC, while the amount of delayed false pulses was investigated by injecting burst electrons to MWPC. MWPC output signals were recorded using a fast-FADC system [3].

We also coated a part of MWPC cathode strip with graphite and checked the effect on the MWPC gains. The cathode is made of aluminum, while graphite has a larger work function than aluminum by about 20%. If the delayed false pulses originate from electron emission at the cathode electrode caused by positive ions hitting it, graphite coating could reduce them.

As an extension of our spectrometer system, we are considering a plastic scintillation fiber-tracker system which can provide additional timing information. We tried to investigate responses of a plastic-scintillation fiber with SiPM readout to burst electrons. We newly developed a special circuit to switch bias voltages from the forward direction to reverse direction according to the burst timing

to see any effects on the slow recovery from the saturation due to burst injection.

RESULTS: Fig. 1 shows delayed false-pulse rate versus gain for a gas mixture of Ar : isobutane : methylal = 75 : 15 : 15. The case of mixing R-134a gas instead of methylal is also included for comparison of which data were taken in previous beam tests. It is seen that methylal is much more effective to reduce false-pulse rates compared to R-134a. The effect of delayed false pulses to momentum measurement is also estimated. For the same gas mixture and HV of 1460 V, the number of false tracks reconstructed from false pulses is expected to be about 0.01 for one year of data taking period and is confirmed to be small enough.

The effect of painting graphite on the aluminum cathode strip on the gains was found to be small, about a 5% level of reduction. As a longer-term plan, we would like to investigate signal-to-noise ratios and explore the possibility of coating the cathode surface with an appropriate material.

As to the response of the fiber-SiPM system with applying switching bias voltages, it was found that the state change of the SiPM due to switching the bias voltages from the forward direction to the reverse direction took rather a long time (about 40 μ s) which was too slow for our application. We need to investigate some more details of time evolution of semi-conductor states resulting from bias voltage switching.

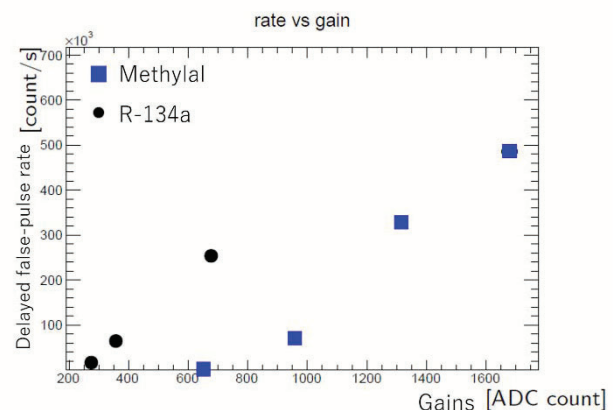


Fig. 1 Relation between the gain and the delayed false-pulse rate.

REFERENCES:

- [1] N. Teshima on behalf of the DeeMe Collaboration, “DeeMe experiment to search for muon to electron conversion at J-PARC MLF”, in proceedings of NUFACT conference PoS (NuFact2017) 109 (2018).
- [2] H. Natori, *et al.*, “A fast high-voltage switching multi-wire proportional chamber”, Prog. Theor. Exp. Phys. 2017(2) 023C01 (2017).
- [3] N.M. Truong, *et al.*, “Real-Time Lossless Compression of Waveforms Using an FPGA”, IEEE Trans. Nucl. Sci. 65 2650 (2018).

CO12-14 Determination of Impurity Metals in the Uranium Oxide by ICP-MS

T. Miura¹, K. Takamiya², Y. Iinuma², H. Yoshinaga²

¹National Metrology Institute of Japan, AIST

²Institute for Integrated Radiation and Nuclear Science, Kyoto University

INTRODUCTION: National Metrology Institute of Japan (NMIJ) is responsible for developing certified reference materials and for establishing the traceability of SI (The International System of Units) on chemical metrology in Japan. To establish SI traceability, the starting material of inorganic standard solution should be characterized and measured impurities by sensitive analytical method. In this study, the impurity metals in the uranium oxide reagent were measured by inductively coupled plasma mass spectrometry (ICP-MS) for assist the development of precise titration method for uranium.

EXPERIMENTS: The 0.2 g of uranium oxide reagent was weighed in the 200 mL borosilicate glass beaker. The weighed uranium oxide sample was dissolved by 5 mL of 69 % HNO₃. After dissolution of the uranium oxide reagent, the solution was diluted by 1 % HNO₃ and transfer to the 100 mL PFA (Perfluoroalkoxy alkane) bottle. Two samples (1.0 g and 0.98 g) were taken from the prepared sample solution. The sample solutions were evaporated to dryness using hot plate. After evaporation, the residue was dissolved with 20 mL 4 mol dm⁻³ HNO₃. The sample solutions were loaded on eichrom U/TEVA extraction chromatographic resin column (bed volume; 2 mL) that had been previously washed with 10 mL of 4 mol dm⁻³ HNO₃. The U/TEVA resin [1] column was then washed with 10 mL 4 mol dm⁻³ HNO₃ and 20 mL 5 mol dm⁻³ HCl. The Al, Mn, Fe, Bi, etc. on the U/TEVA resin column were eluted out with 10mL 4M nitric acid as the first washing solution, and then Th was eluted from the U/TEVA resin column with 20mL 5 mol dm⁻³ HCl as the second washing solution. The effluent at sample loading solution, 1st washing solution (10 mL 4 mol dm⁻³ HNO₃) and 2nd washing solution (20 mL 5 mol dm⁻³ HCl) combined and evaporated to dryness using hot plate. Then the residue was dissolved with 1 % HNO₃. The sample solutions were transferred to 50 mL polypropylene bottles. The sample solutions were introduced to determine the impurity metals by Analytic-jena PlasmaQuant ICP-MS. The operating conditions for the ICP-MS were shown in Table 1.

Table 1 Operating conditions for the ICP-MS

	ICP source operation parameters
RF power	1.2 kW
Plasma gas flow	9.0 L/min
Auxiliary gas flow	1.5 L/min
Nebulizer gas flow	1.0 L/min
Nebulizer	Borosilicate glass concentric

The NIST SRM standard solutions (Sc, La, Ce, Nd, Pr, Sm, Eu, Gd, Tb, Dy, Ho, Er, Tm, Yb, and Lu), SPEX XSTC-7, SPEX XSTC-22, SPEX XSTC-331 were used for calibration of the ICP-MS.

RESULTS: The analytical results of impurity metals were shown in Table 2. The

Table 2 Analytical results of metallic impurity elements in the uranium oxide reagent

	Analytical results		Analytical results
Sc	< 50 mg/kg	Pr	< 9 mg/kg
V	< 70 mg/kg	Nd	< 10 mg/kg
Cr	< 15 mg/kg	Sm	< 4 mg/kg
Mn	< 1 g/kg	Eu	< 2 mg/kg
Fe	< 0.1 g/kg	Gd	< 5 mg/kg
Co	< 12 mg/kg	Tb	< 4 mg/kg
Zn	< 35 mg/kg	Dy	< 8 mg/kg
Ga	< 19 mg/kg	Ho	< 14 mg/kg
Sr	< 11 mg/kg	Er	< 30 mg/kg
Y	< 6 mg/kg	Tm	< 9 mg/kg
Zr	< 50 mg/kg	Yb	< 2 mg/kg
Mo	< 11 mg/kg	Lu	< 10 mg/kg
Pd	< 23 mg/kg	Hf	< 3 mg/kg
Cd	< 9 mg/kg	Pt	< 16 mg/kg
Sn	< 40 mg/kg	Tl	< 7 mg/kg
Ba	< 6 mg/kg	Pb	< 0.5 g/kg
La	< 5 mg/kg	Bi	< 2 mg/kg
Ce	< 10 mg/kg	Th	< 16 mg/kg

REFERENCES:

[1] E. P. Horwitz *et al.*, Anal. Chim. Acta, 266, 25-37, 1992.

CO12-15 Neutron activation of medicines for development of new imaging methodology

A. Toyoshima, N. Koshikawa¹, Y. Kadonaga², A. Omata¹, M. Masubuchi¹, K. Tokoi³, A. Imada⁴, K. Takamiya⁵, and J. Kataoka¹

Institute for Radiation Sciences, Osaka University

¹*Graduate School of Advanced Science and Engineering, Waseda University*

²*Graduate School of Medicine, Osaka University*

³*Graduate School of Science, Osaka University*

⁴*School of Science, Osaka University*

⁵*Institute for Integrated Radiation and Nuclear Science, Kyoto University*

INTRODUCTION: In the drug delivery system, it is desired to obtain high therapeutic effects with no side-effect by direct transportation of medicine to lesion. At present, it is impossible to simultaneously evaluate the accumulation of administrated medicine in a targeted organ and its therapeutic effect without incision. Imaging of radiations emitted from activated medicine, however, makes it possible to visualize the pharmacokinetics without incision. In our group, an advanced imaging camera available for a wide energy range of X- and γ -rays has been already developed [1]. In this study, therefore, we activated gold nano-particle (AuNP), platinum nano-particle (PtNP), Cisplatin, and Gadoteridol by thermal neutron to produce short-lived radioisotopes suitable for imaging: ^{198}Au (half-life = 2.69 d), ^{159}Gd (18.48 h), and ^{197}Pt (18.3 h). This study is our first approach to develop a novel methodology of the radioactivated medicine imaging.

EXPERIMENTS: For AuNP, PtNP, and Gadoteridol, dried samples were separately prepared by evaporation of their commercial products on filter papers which were then enclosed in small plastic bags. For Cisplatin, its powder was enclosed in a plastic bag. The prepared AuNP (0.3 mg), Gadoteridol (1 mg), PtNP (2 mg), and Cisplatin (5 mg) samples were irradiated by thermal neutron using the Pn-2 pneumatic transport system of KUR for 1 min, 10 min, 20 min, and 20 min, respectively. After the irradiation, these were transported to Osaka University. Experiments of PtNP and Cisplatin were carried out 1 day after the irradiation for the decay of simultaneously produced detection-hindering radioisotope ^{199}Pt with a shorter half-life (30.8 min). Gamma rays from the samples were measured using a high purity Ge detector. For AuNP and PtNP, purification by filtration was made after suspension. For Gadoteridol and Cisplatin, HPLC analysis/separation was carried out after dissolution. After the separation, measurement for the purified samples was also conducted using the imaging camera [1].

RESULTS: In the measurements using the Ge detector, γ -rays of ^{198}Au (412 keV), ^{159}Gd (364 keV), ^{197}Pt (77 keV) were identified in the AuNP, Gadoteridol, and both PtNP and Cisplatin samples, respectively. In Fig. 1, γ -ray

spectrum of AUNP is showed as an example. Two γ -peaks of ^{198}Au and characteristic X-rays from Hg after the β^- decay of ^{198}Au are clearly seen. This means that the irradiated AuNP was activated as intended. For the activated samples, the amounts of the radioisotopes at the γ -ray measurements were determined to be approximately 100 kBq for ^{198}Au in AuNP, 70 kBq for ^{159}Gd in Gadoteridol, 15 kBq for ^{197}Pt in PtNP, and 70 kBq for ^{197}Pt in Cisplatin. Results on the purification of AuNP and PtNP, HPLC analysis of Gadoteridol and Cisplatin, and imaging of the activated samples are under analysis.

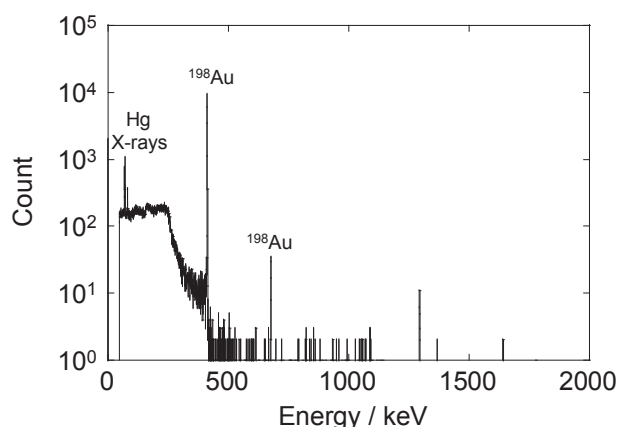


Fig. 1. Gamma ray spectrum of the activated AuNP measured with a high purity Ge detector.

REFERENCE:

[1] A. Omata *et al.*, *Sci. Reports*, **10** (2020), 14604.

CO12-16 Evaluation Test of Quantitative 3-D Measurement of Gamma Dose in the Reactor Building by ETCC

T.Tanimori¹, S.Sonoda¹, A.Takada¹, M.Tsuda¹,
K.Tahara¹, K.Kobayasi¹, H.Nagai², T.Sato²,
H.Nakayama², M.Tanigaki³, A.Taniguchi³

¹Graduate School of Science, Kyoto University

²Nuclear Science and Engineer Center, JAEA

³Institute for Integrated Radiation and Nuclear Science, Kyoto University

INTRODUCTION: We have developed an electron track detecting Compton camera (ETCC) that can uniquely determine the direction of arrival of MeV gamma rays. The ETCC is the unique gamma ray camera that can acquire linear images by bijective method as well as an optical camera, and thus can measure 3-D dose rates distribution from at least two directions simultaneously. On the other hand, conventional Compton cameras or multi-pinhole cameras cannot measure such quantitative 3D dose distribution due to their nonlinear images.

To demonstrate this, 3D measurements of the 1F (1st Fukushima Nuclear Power Plant) reactor building was scheduled in 2021 in the project of “Nuclear Energy Science & Technology and Human Resource Development Project” supported by JAEA. However, due to the coronal disaster, it has been impossible to carry out the measurement in 1F by the end of December 2021, when the project was to be terminated. Therefore, we proposed the 3D dose rate measurement in the reactor facility of this institute, which is the only facility in Japan that can be used jointly.

Method

The ETCC was set on the second-floor catwalk of the reactor building looking down on the reactor and measuring the reactor from four directions, 70 to 120 degrees apart in Fig.1. The average dose on the catwalk at 5 MW output is about 2 μ Sv/h. The 20 cm diameter ETCC to be used in this experiment has a detection efficiency of about 0.02% for 662 eV gamma radiation after noise reduction by analy-



Fig. 1 20cmETCC set on catwalk.

sis. Therefore, at this dose rate, 5 counts of gamma rays of which direction is determined completely per second can be obtained. To obtain a 3D dose distribution with an accuracy of 5 degrees cubic in space, we need at least 50,000 gamma rays per direction, which means that 2-4 hours observation at one direction is needed. Considering the operation time of 6hours at 5MW operation in one day, 3 days observation are needed.

EXPERIMENTS AND RESULTS:

The experiment was done at 5 WM output on December 2, 9, and 16. We measured the reactor from four different directions and obtained gamma-ray images with the energy range from 0.1 to 5 MeV. The data are currently being analyzed. It is already well known that when the reactor power is increased to 5 MW, the air inside the reactor is irradiated and ⁴¹Ar was produced. Then, a small amount of ⁴¹Ar was emitted outside the reactor. ⁴¹Ar emits 1290 keV γ -rays with a half-life of 110 minutes. Because the dose of ⁴¹Ar is so small, the details of how it exits from the reactor have long been unknown. From the catwalk in front of the control room, we measured the image of 1290 keV gammas after 10:00 a.m., when ⁴¹Ar was

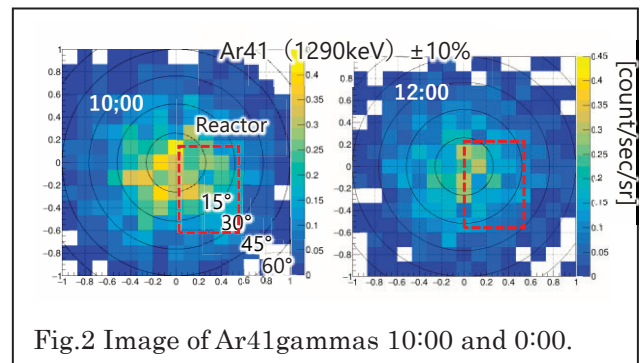


Fig.2 Image of Ar41gammas 10:00 and 0:00.

strongest, and at 12:00 a.m., when the half-life had elapsed, as shown in Fig.2, ⁴¹Ar was clearly measured to be decreasing. In fact, changes of ⁴¹Ar at intervals of 7 minutes were also captured, and we succeeded in capturing the diffusion of ⁴¹Ar as an animation. Currently, we are seeking the distribution of gamma rays in other energy regions and their three-dimensional distributiona.